PHYSICAL REVIEW B **87**, 100101(R) (2013)

Codetermination of crystal structures at high pressure: Combined application of theory and experiment to the intermetallic compound $AuGa_2$

B. K. Godwal,[1] S. Stackhouse,[2] J. Yan,[3] S. Speziale,[4] Burkhard Militzer,[1,5] and R. Jeanloz[1,5]
[1]*Department of Earth and Planetary Science, University of California Berkeley, California 94720, USA*
[2]*School of Earth and Environment, University of Leeds, LS2 9JT, United Kingdom*
[3]*Advanced Light Source, Lawrence Berkeley National Laboratory, Berkeley California 94720, USA*
[4]*Deutsches GeoForschungsZentrum, Section 3.3, Telegrafenberg, 14473, Potsdam, Germany*
[5]*Miller Institute for Basic Research in Science and Department of Astronomy, University of California Berkeley, California 94720, USA*

(Received 25 June 2012; revised manuscript received 7 November 2012; published 21 March 2013)

A combination of x-ray diffraction at high pressures and first-principles calculations reveals the sequence of crystal-structural phase transitions in $AuGa_2$ from cubic ($Fm\overline{3}m$) to orthorhombic ($Pnma$) at 10 (± 4) GPa and then to monoclinic ($P2_1/n$) at 33 (± 6) GPa. Neither theory nor experiment would have been adequate, on their own, in documenting this sequence of phases, but together they confirm a sequence differing from the $Fm\overline{3}m \rightarrow Pnma \rightarrow P6_3/mmc$ transitions predicted for CaF_2 and $Pnma \rightarrow P112_1/a$ transition reported for $PbCl_2$ and $SnCl_2$. The combined results from theory and experiment also allow us to constrain the equations of state of the three phases of $AuGa_2$. Calculations on the analog $PbCl_2$ predict a transition to the $P2_1/n$ phase seen in $AuGa_2$ that could, therefore, be a common high-pressure phase for $PbCl_2$-structured compounds.

DOI: 10.1103/PhysRevB.87.100101 PACS number(s): 61.50.Ks, 71.10.Hf, 64.30.−t, 71.20.−b

There is considerable interest in AX_2 ($A = \mathrm{Au}$, $X = \mathrm{In, Ga}$) -type intermetallic compounds, because of their technological importance and unique physical properties, including superconductivity at low temperatures.[1,2] Their electrical resistivity, Hall coefficients, lattice and electronic specific heats, and Fermi surfaces are similar.[1] However, the Ga Knight shift, spin-lattice relaxation times, and magnetic susceptibility of $AuGa_2$ all show strong temperature dependence between 20 and 300 K.[3] Also, the Seebeck coefficient of $AuGa_2$ reverses sign at 14 and 145 K, and the elastic behavior exhibits a large temperature dependence around 85 K.[4] These anomalies are not shared by the isostructural $AuAl_2$ and $AuIn_2$, suggesting differences in bonding character that we explore through the use of pressure.

The intermetallic compounds $AuGa_2$, $AuIn_2$, $AuAl_2$, and ACl_2 (A = Pb, Sn) have the fluorite-type structure ($Fm\overline{3}m$) at ambient conditions. Experimental studies indicate that the structural prototype CaF_2 transforms to an orthorhombic $PbCl_2$-cotunnite-type structure ($Pnma$) at around 8 GPa,[5] and first-principles calculations show a $Fm\overline{3}m \rightarrow Pnma \rightarrow P6_3/mmc$ structural sequence under pressure.[6] A monoclinic postcotunnite structure ($P112_1/a$) has also been found by Leger *et al.* for ACl_2 (A = Pb, Sn) compounds,[7] and by Godwal *et al.* for $AuIn_2$.[8] In the present work we provide a method to obtain the structure of unknown phases at high pressures from powdered samples and look at the structural behavior of $AuGa_2$ under pressure and compare it with existing studies on $AuIn_2$ and $AuAl_2$.

Sample preparation and initial characterization have been described previously.[9] Briefly, single-phase cubic $AuGa_2$ ($Fm\overline{3}m$), with lattice parameter 6.077 (± 0.001) Å corresponding to a unit-cell volume of 224.5 (± 0.1) Å^3, was ground to 5–10-μm average grain size; the powder was then loaded into a ~120-μm-diameter sample chamber drilled out of a 250-μm-thick stainless-steel foil that had been indented to a final thickness of ~45 μm. The sample was compressed between two diamond anvils with 230-μm culets, using a methanol-ethanol-water mixture (16:3:1 volume ratio) as pressure-transmitting medium. A few specks of ruby were loaded for pressure calibration. High-pressure experiments were performed using a symmetric diamond-anvil cell (DAC) at beamline 12.2.2 of the Advanced Light Source at Lawrence Berkeley National Laboratory.[10] X-ray powder-diffraction patterns were collected in angle-dispersive geometry, using monochromatic radiation of wavelength $\lambda = 0.4959$ (± 0.0004) Å and a MAR345 image-plate detector placed at a distance of 237.6 (± 0.1) mm from the sample. The x-ray beam width was approximately 30 μm both in horizontal and vertical directions.

All experiments were performed at room temperature, and pressure was determined from ruby fluorescence.[11] The sample-to-detector distance, image center, and detector tilt were calibrated by collecting the diffraction pattern of powdered LaB_6 at ambient conditions. The software package FIT2D (Ref. 12) was used both for beam-position and sample-to-detector distance calibrations, and to integrate the two-dimensional diffraction images to obtain one-dimensional patterns.

X-ray-diffraction patterns with increasing pressure show that $AuGa_2$ undergoes structural phase transitions at 14 (± 0.7) and 35 (± 1.5) GPa (Fig. 2 in Ref. 13). Under decompression, the monoclinic phase transforms back to the orthorhombic phase at about 35 GPa, which remains metastable to 8 GPa or less. Upon full release of pressure, we observe the ambient cubic ($Fm\overline{3}m$) phase. From observations on compression and decompression, we estimate the transition pressures to be 10 (± 4) GPa and 33 (± 4) GPa, respectively. These results are consistent with previous work identifying a structural phase transition near 8 GPa,[9] and are also in accord with the notion that nonhydrostatic conditions can reduce kinetic hindrances for pressure-induced phase transitions.[14]

We employed the software package EXPO (Ref. 15) to index the powder-diffraction patterns, and to determine the structure and unit-cell parameters for the two high-pressure polymorphs of $AuGa_2$ observed in our experiments. The program indexed the diffraction patterns of the intermediate and high-pressure phases as possible orthorhombic and monoclinic cells, respectively, but failed to uniquely determine the structures due to variable peak intensities affecting the structure determination and Rietveld analysis.

In view of this, we employed calculations based on density functional theory to predict the structural sequence under pressure, using a strategy similar to that adopted in Ref. 16. We performed total-energy calculations as a function of pressure for each of the polymorphic structures proposed from theory and experiments for these and related CaF_2 compounds.[5–8] All calculations were performed using the VASP code,[17,18] employing the projector-augmented-wave method.[19,20] The potentials were generated using valence configurations of s^1d^{10} for Au and $4s^2p^1$ for Ga. For all results presented here, the exchange-correlation functional adhered to the local-density approximation (LDA),[21] but for comparison purposes we also performed test calculations using the PBE formulation of the generalized gradient approximation (GGA).[22] The kinetic-energy cutoff for the plane-wave expansion was 600 eV, and Brillouin-zone sampling was performed using special k-point grids[23] (cubic phase: $12 \times 12 \times 12$; orthorhombic phase: $8 \times 14 \times 6$; hexagonal phase: $12 \times 12 \times 12$; and postcotunnite phase: $6 \times 8 \times 18$). These settings ensure that calculated volumes converge to within 0.1 $Å^3$ and enthalpies to less than 1 meV per atom. Scalar relativistic effects were accounted for, but spin-orbit coupling was neglected.

Upon optimization, the postcotunnite ($P112_1/a$) phase observed by Leger *et al.* in ACl_2 (A = Sn, Pb) compounds[7] transformed to an orthorhombic (*Pnma*) structure, resembling the hypothetical Co_2Si-type structure also discussed by these authors. Enthalpies calculated for this phase are labeled "orthorhombic 2 (*Pnma*)." In addition, initial optimization of the orthorhombic $PbCl_2$-type structure, using a 400-eV cutoff and $6 \times 10 \times 4$ k-point grid, resulted in the evolution of a monoclinic ($P2_1/n$) structure at 40 GPa. Further calculations were performed for this structure using a cutoff of 600 eV and an $8 \times 18 \times 6$ k-point grid, and the results are shown as "monoclinic ($P2_1/n$)." Lattice parameters and atomic co-ordinates for all phases are provided (see Table II in Ref. 13 and also Ref. 24). The calculated enthalpies suggest a transition from cubic ($Fm\bar{3}m$) to orthorhombic (*Pnma*) structures at about 14 GPa and from orthorhombic (*Pnma*) to monoclinic ($P2_1/n$) structures at about 32 GPa (Fig. 1), both in agreement with the experimental observations. The optimized structural parameters for the orthorhombic and monoclinic structures, close to the transition pressures, are listed in Table I. The corresponding phase-transition pressures calculated using the GGA were 12 and 25 GPa. That the GGA values are lower than the LDA values is unusual, going against the more general observation that transition pressures calculated using the LDA are lower than those calculated using the GGA. This could be related to our neglect of spin-orbit coupling.

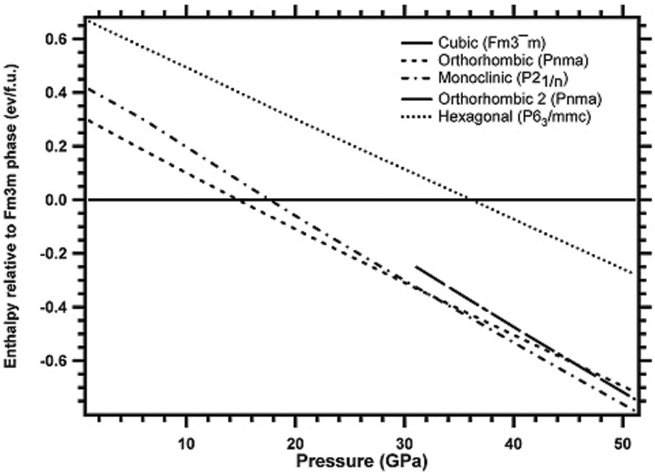

FIG. 1. Calculated enthalpies of all phases studied, relative to that of the cubic ($Fm\bar{3}m$) structure. The computed enthalpies suggest a transition from the cubic ($Fm\bar{3}m$) to orthorhombic (*Pnma*) phase at about 14 GPa and from the latter to the monoclinic ($P2_1/n$) phase at about 32 GPa.

The equilibrium volume, bulk modulus, and its pressure derivative (Table II) are estimated for the cubic, orthorhombic, and monoclinic phases from the P-V equations of state obtained from total-energy calculations as a function of volume (see Ref. 13). Good agreement is found with the results of earlier calculations,[25,26] and reasonable agreement with present and previous experimental data.[4] The equations of state calculated using the GGA are in poor agreement with the experimental measurements. In view of this, as well as the fact that previous theoretical studies have shown the LDA to determine the properties of cubic $AuGa_2$ better than the GGA,[25,26] we report results for the LDA calculations.

We used the optimized atomic coordinates as the initial values for Rietveld refinement of the experimental data for both observed high-pressure phases.[27,28] The refined patterns close to the phase transitions are shown in Fig. 2. Good agreement is seen between the calculated and observed patterns. The cell parameters and final fractional atomic coordinates for cubic to orthorhombic and orthorhombic to monoclinic phase transitions are given in Table I of Ref. 13.

The measured P-V data (Fig. 3) show three regions, corresponding to the cubic ($Fm\bar{3}m$), orthorhombic (*Pnma*),

TABLE I. Calculated structural parameters of high-pressure phases.

Orthorhombic (*Pnma*) at 16 GPa	Monoclinic ($P2_1/n$) at 35 GPa
$a = 6.764$ Å, $b/a = 0.500$, $c/a = 1.180$	$a = 6.497$ Å, $b/a = 0.439$, $c/a = 1.387$
$\alpha = \beta = \gamma = 90^\circ$	$\alpha = \beta = 90^\circ$, $\gamma = 77.778^\circ$
Au ($4c$) : (0.252,0.250, 0.653)	Au 1 ($4e$) : (0.235, 0.438, 0.379)
Ga 1 ($4c$) : (0.876,0.250, 0.560)	Ga 1 ($4e$) : (0.899, 0.105, 0.375)
Ga 2 ($4c$) : (0.444, 0.250, 0.358)	Ga 2 ($4e$) : (0.433, 0.216, 0.626)

TABLE II. Calculated equation of state parameters for cubic, orthorhombic, and monoclinic phases. The experimental values of bulk modulus (K) and its derivative (K') are based on G vs g fit.

	V_0 (Å^3)	K (GPa)	K'
		Cubic ($Fm\bar{3}m$)	
LDA (this work)	219.47	95.10	5.59
LDA (Ref. 27)	219	87.4	5.620
LDA (Ref. 28)	219	96	
GGA (Ref. 28)	241	69	
Experimental (this work)	224.5 ($\pm$0.1)	81 ($\pm$5)[a]	11 ($\pm$2)
		Orthorhombic ($Pnma$)	
LDA (this work)	204.79	95.97	5.24
Experimental (this work)	204.0 ($\pm$1.0)	112.0 ($\pm$12)	(5 $\pm$ 1)
		Monoclinic ($P2_1/n$)	
LDA (this work)	201.08	98.55	5.19
Experimental (this work)	192.0 ($\pm$4)	157.0 ($\pm$5)[b]	4.0

[a] Our data points at 1.9 and 2.6 GPa are perfectly compatible with ultrasonic value of bulk modulus (Ref. 4) and with data below 6 GPa from Ref. 9 (see (Ref. 16).

[b] The combined K and K' values from theory are found to be compatible with experimental volumes.

and monoclinic ($P2_1/n$) phases. A weighted least-squares fit of Birch's normalized pressure as a function of Eulerian strain (F vs f) for the cubic phase, with fixed initial volume V_0 of 224.5 ($\pm$0.1) Å^3, resulted in bulk-modulus and pressure-derivative values of $K_{T0} = 81$ ($\pm$5) GPa and $(\partial K_T/\partial P)_{T0} = 11$ ($\pm$2) (see Refs. 13 and 29). The derived K_{T0} agrees with extant zero-pressure ultrasonic data (isentropic bulk modulus, $K_{S0} =$ 82 GPa),[4] and the isothermal compression curve is consistent with the results of a previous static-compression study.[9]

The parameters of the equation of state based on experimental data are in *apparent* disagreement with those from our DFT calculations (Table II), and with earlier computational studies.[9,26] However, the disagreement between experiments and computations presented can be explained in terms of theory's underestimation of equilibrium volumes (typical of the LDA). A correction was estimated using the method of Oganov *et al.*,[30] but neglecting the thermal pressure term (considered as negligible at ambient conditions). The calculated pressure shift (2 GPa) moves the isothermal compression curves to higher pressure, in accord with experimental values (see Fig. 3).

In addition, previous studies show that the cubic phase of $AuGa_2$ may be subject to an electronic topological transition (ETT) causing an anomalous change of the pressure dependence of the bulk modulus below 6 GPa.[9,31] Our experimental results for the low-pressure phase below 6 GPa are compatible with the equation of state based on computations, and this could confirm the presence of an anomaly in the compression curve (see Ref. 13).

As the initial volumes for the orthorhombic and monoclinic phases are not known, we analyzed the pressure-volume data (Fig. 3) using an alternative approach based on the fit of normalized pressure G versus Eulerian finite-strain g.[29] The G vs g fit has the merit of allowing the refinement of equation-of-state parameters when the initial volume V_0 is unknown.[29] The G vs g fit yields $V_0 = 204$ ($\pm$1) Å^3, $K_{T0} = 112$ ($\pm$10) GPa, and $(\partial K_T/\partial P)_{T0} = 5$ ($\pm$1) for the intermediate orthorhombic phase, in agreement with theory (see Table II). The G vs g analysis for the high-pressure phase does not reliably constrain the value of the bulk modulus and pressure derivative $(\partial K_T/\partial P)_{T0}$ because of the limited range of strain spanned by the data. A linear G vs g fit [corresponding to a second-order Eulerian equation of state, with $(\partial K_T/\partial P)_{T0} = 4$] yields $V_0 = 192$ ($\pm$9) Å^3—marginally compatible with computational results—and $K_{T0} = 157$ ($\pm$5) GPa, in disagreement with theory (see Table II). However, the discrepancy between experiments and calculations for K_{T0} and $(\partial K_T/\partial P)_{T0}$ is mostly due to the choice of the second-order equation to fit the experimental data, and the theoretical P-V compression curve is more compatible with the raw experimental data (Fig. 3; see also Fig. 6 and discussion in Ref. 13).

The cubic ($Fm\bar{3}m$) to orthorhombic ($Pnma$) structural phase transition at around 14 GPa is accompanied by a large volume change (7% by computation, 9% from experiments), whereas the transition from orthorhombic ($Pnma$) to monoclinic ($P2_1/n$) phases has a small volume change (~1% by computation, 2% based on the experimental results). The experimental P-V curves follow the corrected theoretical values closely at all pressures (Fig. 3 and Ref. 13).

Lattice dynamics studies of $AuGa_2$ reveal that the TO, LO, and LA phonon modes shift to higher frequencies, while the transverse acoustic (TA) phonon branch along Γ-L softens with increasing pressure, indicating a negative mode Grüneisen parameter.[31] The structural instability resulting from phonon softening should occur with negligible volume change. We suggest that this softening, which is predicted to occur close to 22 GPa, is associated with the orthorhombic to monoclinic phase transition that shows negligible volume change both in theoretical and experimental results. There is also a prediction of another electronic topological transition in $AuGa_2$ close to 7 GPa,[9,13,31] resulting from a topological singularity along the Γ-X direction of the Fermi surface. It is possible that the $Fm\bar{3}m$ to $Pnma$ structural phase transition above 14 GPa in $AuGa_2$ is driven by this ETT.

In the present work, the structural sequence observed for $AuGa_2$ is corroborated by theoretical calculations that indicate

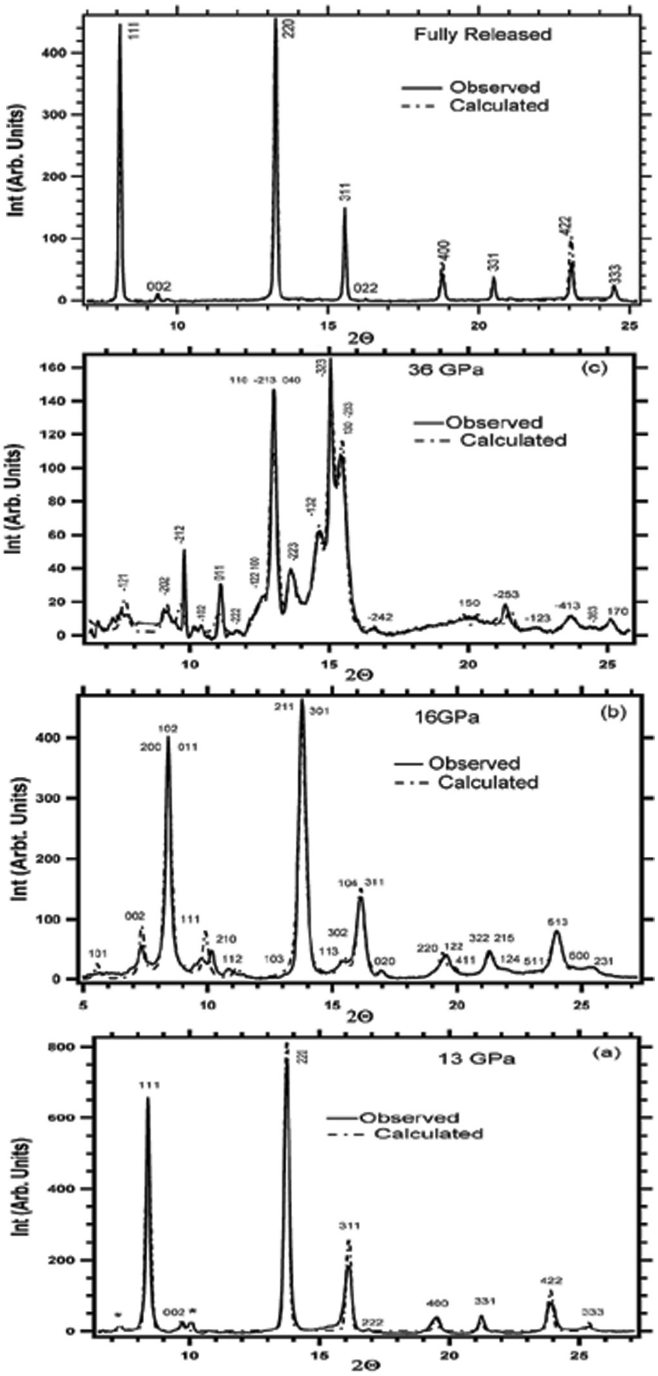

FIG. 2. Comparison of observed and calculated diffraction patterns for the (a) cubic ($Fm\overline{3}m$) at 13 GPa, (b) orthorhombic *(Pnma)* at 16 GPa, and (c) monoclinic ($P2_1/n$) phases at 36 GPa. The pattern for fully decompressed sample (top panel) reveals that $AuGa_2$ transforms back to its ambient $Fm\overline{3}m$ phase. The Rietveld refinement of experimental data was performed using atomic coordinates from the theoretical calculations. The weak peaks indicated by * in (a) are due to orthorhombic phase.

that $AuIn_2$ and $AuAl_2$ transform from cubic to cotunnite to the Co_2Si-type structure, which remains stable up to 3 TPa (the highest pressure studied). This structural sequence is in agreement with the available data on $AuAl_2$,[16,32] and consistent with $AuIn_2$ data.[8,13] While there has been no direct detection of an ETT in $AuIn_2$,[33] electronic structure calculations report an ETT,[8,13,31] and we associate this with the anomaly observed in the compressibility curve data near 3 GPa. No ETT is observed for $AuAl_2$.[31,32] Theoretical studies of the electronic band structure and phonon frequencies of $AuIn_2$ and $AuAl_2$ show no anomalies at higher pressures for either composition,[13,31] suggesting that the cause of the high-pressure structural changes in $AuIn_2$ and $AuAl_2$ differ from that in $AuGa_2$.

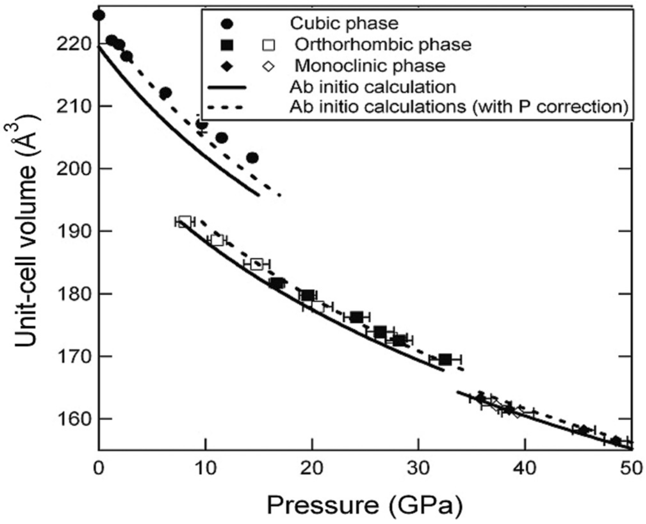

FIG. 3. Experimental unit-cell volumes determined for $AuGa_2$ under static compression. The data show three separate regions: a low-pressure region ($\leqslant 15$ GPa) corresponding to the cubic ($Fm\overline{3}m$) phase, an intermediate-pressure region (8 GPa $\leqslant P \leqslant 35$ GPa) corresponding to the orthorhombic (*Pnma*) phase, and a high-pressure region (>35 GPa) corresponding to the monoclinic ($P2_1/n$) phase. The filled and open symbols represent compression and decompression, respectively. The dashed and solid lines are the *P-V* compression curves from theory with and without pressure correction, respectively.

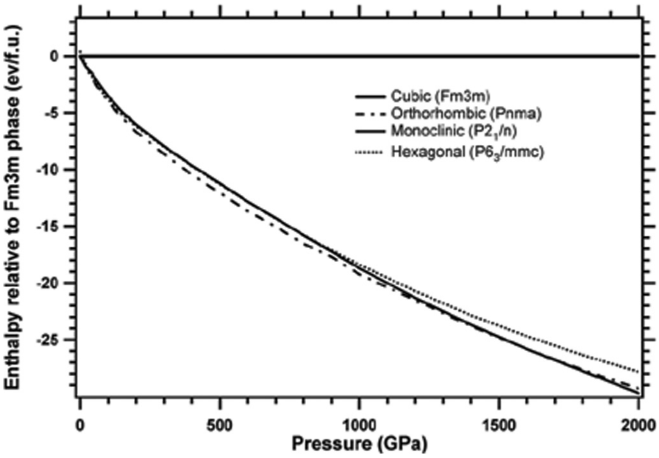

FIG. 4. Calculated enthalpies of all phases of $PbCl_2$ studied, relative to that of the cubic ($Fm\overline{3}m$) structure. The calculations suggest a displacive transition from the ambient orthorhombic structure (*Pnma*) to the Co_2Si-type structure (*Pnma*) at low pressure and then to the monoclinic ($P2_1/n$) phase at about 1600 GPa. Metallization begins at about 100 GPa.

The postcotunnite ($P112_1/a$) phase is claimed to be the final step in the structural sequence for AX_2 compounds by Leger *et al.*[7] Since we found this phase unstable in $AuGa_2$ we performed further calculations for $PbCl_2$. The potentials were generated using valence configurations of $d^{10}s^2p^2$ for Pb and s^2p^5 for Cl. The kinetic-energy cutoff for the plane-wave expansion was 600 eV, and Brillouin-zone sampling was performed using special k-point grids identical or similar to those for $AuGa_2$. These settings ensure that calculated volumes converge to within 0.1 Å^3 and enthalpies to less than 1 meV per atom. Similar to our observation for $AuGa_2$, the postcotunnite phase ($P112_1/a$) of $PbCl_2$ was found to be unstable. Instead, our studies indicate a displacive phase transition from the cotunnite phase to a Co_2Si-type structure at low pressure (becoming metallic just over 100 GPa), followed by a transition to the monoclinic ($P2_1/n$) phase at about 1600 GPa (Fig. 4).

This has important implications for the crystal chemistry of AX_2 compounds, as over 400 compounds are isostructural to $PbCl_2$ at ambient conditions, and many transform to the cotunnite structure at high pressure.[7] In view of our findings that postcotunnite structure ($P112_1/a$) is unstable, all these compounds will acquire monoclinic ($P2_1/n$) phase at extreme pressures. The present study's confirmation of the structural sequence highlights the utility of first-principles calculations in supporting the analysis of high-pressure experimental data that would otherwise be difficult to interpret.

The present work was funded by the US Department of Energy, University of California, and the Miller Institute. We also acknowledge the use of high performance computing provided by Advanced Research Computing at the University of Leeds and HECToR, the UK's national high-performance computing service, which is provided by UoE HPCx Ltd at the University of Edinburgh, Cray Inc and NAG Ltd, and funded by the Office of Science and Technology through EPSRC's High End Computing Programme.

---

[1] J. H. Wernick, A. Menth, T. H. Geballe, G. Hull, and J. P. Maita, J. Phys. Chem. Solids **30**, 1949 (1969).

[2] R. E. Hahn and B. O. Seraphin, Phys. Thin Films **10**, 1 (1978).

[3] V. Jaccarino, W. E. Blumberg, and J. H. Wernick, Bull. Am. Phys. Soc. **6**, 104 (1961).

[4] L. R. Testardi, Phys. Rev. B **1**, 4851 (1970).

[5] K. F. Seifert and B. Bunsenges, Phys. Chem. **70**, 1041 (1966).

[6] X. Wu, S. Qin, and Z. Wu, Phys. Rev. B **73**, 134103 (2006).

[7] J. M. Leger, J. Haines, and A. Atouf, Phys. Rev. B **51**, 3902 (1995).

[8] B. K. Godwal, S. Speziale, M. Voltolini, R. Wenk, and R. Jeanloz, Phys. Rev. B **82**, 064112 (2010).

[9] A. B. Garg, A. K. Verma, V. Vijayakumar, R. S. Rao, and B. K. Godwal, J. Phys.: Condens. Matter **18**, 8523 (2006).

[10] M. Kunz, A. A. MacDowell, W. A. Caldwell, D. Cambie, R. S. Celestre, E. E. Domning, R. M. Duarte, A. E. Gleason, J. M. Glossinger, N. Kelez, D. W. Plate, T. Yu, J. M. Zaug, H. A. Padmore, R. Jeanloz, A. P. Alivisatos, and S. M. Clark, J. Synchrotron Radiat. **12**, 650 (2005).

[11] H. K. Mao, J. Xu, and P. M. Bell, J. Geophys. Res. B **91**, 4673 (1986).

[12] A. P. Hammersley, S. O. Svensson, M. Hanfland, A. N. Fitch, and D. Hausermann, High Press. Res. **14**, 235 (1996).

[13] See Supplemental Material at http://link.aps.org/supplemental/10.1103/PhysRevB.87.100101 for analysis of pressure-volume data to determine equation of state of three polymorphs of $AuGa_2$ and pressure induced bonding changes in $AuGa_2$ and their comparison with $AuIn_2$ and $AuAl_2$.

[14] A. K. Verma, P. Modak, R. S. Rao, B. K. Godwal, and R. Jeanloz, Phys. Rev. B **75**, 014109 (2007).

[15] A. Altomare, M. C. Burla, M. Camalli, B. Carrozzini, G. L. Cascarano, C. Giacovazzo, A. Guagliardi, A. G. G. Moliteri, G. Polidori, and R. Rizzi, J. Appl. Crystallogr. **32**, 339 (1999).

[16] A. K. Verma, P. Modak, and S. M. Sharma, J. Phys.: Condens. Matter **20**, 325215 (2008).

[17] G. Kresse and J. Furthmüller, Comput. Mater. Sci. **6**, 15 (1996).

[18] G. Kresse and J. Furthmüller, Phys. Rev. B **54**, 11169 (1996).

[19] P. E. Blöchl, Phys. Rev. B **50**, 17953 (1994).

[20] G. Kresse and D. Joubert, Phys. Rev. B **59**, 1758 (1999).

[21] J. P. Perdew and A. Zunger, Phys. Rev. B **23**, 5048 (1981).

[22] J. P. Perdew, K. Burke, and M. Ernzerhof, Phys. Rev. Lett. **77**, 3865 (1996).

[23] J. D. Pack and H. J. Monkhorst, Phys. Rev. B **16**, 1748 (1977).

[24] H. T. Stokes, D. M. Hatch, and B. J. Campbell, Computer Code ISOTROPY, Brigham Young University, Provo, UT, 2012.

[25] G. Ügur and F. Doyalp, J. Phys.: Condens. Matter **18**, 6777 (2006).

[26] L.-S. Hsu, Y.-K. Wang, Y.-L. Tai, and J.-F. Lee, Phys. Rev. B **72**, 115115 (2005).

[27] A. C. Larson and R. B. Von Dreele, Los Alamos National Laboratory Report No. LAUR 86-748, 2004.

[28] L. Lutterotti, S. Matthies, H. R. Wenk, A. J. Schultz, and J. W. Richardson, J. Appl. Phys. **81**, 594 (1997).

[29] R. Jeanloz, Geophys. Res. Lett. **8**, 1219 (1981).

[30] A. R. Oganov, J. P. Brodholt, and G. D. Price, Earth Planet. Sci. Lett. **184**, 555 (2001).

[31] Q. Li, Y. Li, T. Cui, Y. Wang, L. J. Zhang, Y. Xie, Y. L. Niu, Y. M. Ma, and G. T. Zou, J. Phys.: Condens. Matter **19**, 425224 (2007).

[32] A. B. Garg, A. K. Verma, V. Vijayakumar, R. S. Rao, and B. K. Godwal, Phys. Rev. B **72**, 024112 (2005).

[33] I. F. Lifshitz, Sov. Phys. JETP **11**, 1130 (1960).